Letter

Quantum chaos and the correspondence principle

Jiaozi Wang [1,2,*] Giuliano Benenti [3,4,5,†] Giulio Casati,[3,6,‡] and Wen-ge Wang [1,§]

[1]*Department of Modern Physics, University of Science and Technology of China, Hefei 230026, China*

[2]*Department of Physics, University of Osnabrück, D-49069 Osnabrück, Germany*

[3]*Center for Nonlinear and Complex Systems, Dipartimento di Scienza e Alta Tecnologia, Università degli Studi dell'Insubria, via Valleggio 11, I-22100 Como, Italy*

[4]*Istituto Nazionale di Fisica Nucleare, Sezione di Milano, via Celoria 16, I-20133 Milano, Italy*

[5]*NEST, Istituto Nanoscienze-CNR, I-56126 Pisa, Italy*

[6]*International Institute of Physics, Federal University of Rio Grande do Norte, Campus Universitário - Lagoa Nova, CP 1613, Natal, Rio Grande Do Norte 59078-970, Brazil*

(Received 17 November 2020; accepted 2 March 2021; published 26 March 2021)

The correspondence principle is a cornerstone in the entire construction of quantum mechanics. This principle has been recently challenged by the observation of an early-time exponential increase of the out-of-time-ordered correlator (OTOC) in classically nonchaotic systems [E. B. Rozenbaum *et al.*, Phys. Rev. Lett. **125**, 014101 (2020)]. Here, we show that the correspondence principle is restored after a proper treatment of the singular points. Furthermore, our results show that the OTOC maintains its role as a diagnostic of chaotic dynamics.

DOI: 10.1103/PhysRevE.103.L030201

Introduction. Since the beginning of quantum chaos investigations, it has been shown that exponentially unstable classical motion can persist in quantum mechanics only up to the Ehrenfest timescale $t_E \propto |\ln \hbar|$ [1], where $\hbar$ is the effective Planck's constant. Indeed, as it was illustrated in Ref. [2], quantum "chaotic" motion is dynamically stable. This means that, unlike exponentially unstable classical chaotic motion, in the quantum case errors in the initial conditions propagate only linearly in time. Therefore the quantum diffusion and relaxation process takes place in the absence of exponential instability, up to the Heisenberg timescale t_H which is the minimum time needed to resolve the discreteness of the operative eigenstates [3–5], namely, those states which enter the initial conditions and therefore determine the dynamics. It should be noticed that, even though the timescale t_E is very short, it diverges as $\hbar$ goes to zero and this ensures the transition to classical motion as required by the correspondence principle.

A popular tool to investigate chaos in quantum systems is the four-point out-of-time-order correlator (OTOC) [6–43], which can be defined as the expectation of the square commutator of two operators taken at different times:

$$C(t) = \langle ||[\hat{A}(t), \hat{B}(0)]|^2 \rangle. \tag{1}$$

In relation to OTOC, classical and quantum maps and two-dimensional billiards have been studied in great detail [13,14,19,21,41,42], since they are more easily amenable to theoretical and numerical investigations. The importance of these studies is in that, despite their simplicity, these models exhibit the typical properties of classical and quantum chaos in more general systems.

The analysis of these systems has shown that the short-time behavior of OTOC exhibits an exponential increase at a rate which is twice the Lyapunov exponent of the corresponding classical system. Quite obviously, for integrable systems, or more generally for systems with only linear instability, the initial correspondence between classical and quantum mechanics extends over much longer times.

A recent interesting Letter [40] has introduced a new element which was previously overlooked and that seems to cast some doubts on the generality of the above picture. In that Letter, classical and quantum polygonal billiards have been investigated. While these systems are known to have zero Lyapunov exponent, it has been found that the corresponding quantum billiards display an initial exponential increase of the quantum mechanical OTOC that has no origin in the classical counterpart. Moreover, the growth rate appears to increase as $\hbar$ is decreased. On the other hand, since polygons have zero Lyapunov exponent, then the corresponding classical OTOC does not grow exponentially at any time. The seemingly unavoidable conclusion is a breakdown of the correspondence principle.

This conclusion is very surprising to us and somehow hard to accept. Indeed, the correspondence principle is a cornerstone of the entire construction of quantum mechanics. As remarked by Jammer [44], "In fact, there was rarely in the history of physics a comprehensive theory which owed so much to one principle as quantum mechanics owed to Bohr's correspondence principle." The fundamental implications of this problem require therefore a deep examination. This is the purpose of the present Letter in which we provide convincing evidence that there is no breakdown of the correspondence principle: The initial growth of the quantum OTOC goes over smoothly into the classical one and the agreement takes place

*wangjz@mail.ustc.edu.cn
†giuliano.benenti@uninsubria.it
‡giulio.casati@uninsubria.it
§wgwang@ustc.edu.cn

 ©2021 American Physical Society

up to times which increase as $\hbar$ goes to zero, in accordance with the correspondence principle. The OTOC then remains a useful diagnosis of chaotic dynamics, provided an appropriate average over the initial states is done and singularities in the potential are rounded off below the scale of Planck's cell. Our analysis is based on the triangle map, which exhibits the same qualitative properties, classical and quantum, of triangular or polygonal billiards (in particular, zero Lyapunov exponent and exponential growth of the quantum OTOC), while being much simpler for analytical and numerical investigations. This is crucial in our case where, in order to discuss the classical limit, it is desirable to consider sufficiently small values of $\hbar$.

Before discussing our results, we would like to remark that, while the correspondence principle maintains its validity, the analysis of Ref. [40] allows us to discover an important feature of the quantum-to-classical transition. Indeed, polygons have zero Lyapunov exponent but a round-off of a corner, no matter how small, might lead to chaotic exponentially unstable motion. On the other hand, in a nonconvex polygon, due to the finite size of the quantum packet, the quantum system will always "see" a rounded vertex and therefore will move as in a classically chaotic system. This is the reason for the observed initial exponential growth in nonconvex polygons. The importance of this observation is that a similar phenomenon can take place in generic Hamiltonian systems due to the presence of unstable fixed points which might lead to an exponential increase of OTOC even in integrable systems. This fact may render the role of OTOC to be very delicate in discriminating integrable from chaotic systems. Indeed, in recent papers [37,38] it has been claimed that the exponential growth of OTOC does not necessitate chaos.

Exponential instability in the round-off triangle map. The triangle map [45] is defined on the torus with coordinates $(x, p) \in [-1, 1) \times [-1, 1)$ as follows,

$$\begin{cases} p_{n+1} = p_n - V'(x_n) & (\mathrm{mod}\ 2), \\ x_{n+1} = x_n + p_{n+1} & (\mathrm{mod}\ 2), \end{cases} \tag{2}$$

where $V(x) = -\alpha|x| - \beta$. It is an area preserving, parabolic, piecewise linear map which corresponds to a discrete bounce map for the billiard in a triangle. The map is marginally stable, i.e., initially close trajectories separate linearly with time. Even though the Lyapunov exponent is zero, numerical evidence indicates that this map, for generic, independent irrationals α and β, is ergodic and mixing [45]. Hereafter we consider $\beta = 0$ for simplicity. In this latter case the map is only ergodic [45].

We also consider the round-off triangle map, where we substitute the cusps in the potential $V(x)$ by small circle arcs of radius r (see Fig. 1):

$$\frac{V(x)}{\alpha} = \begin{cases} -\sqrt{2}r + \sqrt{r^2 - x^2}, & |x| \leqslant \frac{\sqrt{2}}{2}r, \\ -1 + \sqrt{2}r - \sqrt{r^2 - (|x| - 1)^2}, & |x| \geqslant 1 - \frac{\sqrt{2}}{2}r, \\ -|x|, & \text{otherwise}. \end{cases} \tag{3}$$

The original triangle map is recovered for $r = 0$.

The round-off triangle map is exponentially unstable for any $r \neq 0$. The Lyapunov exponent can be estimated by considering the tangent map. The length of the tangent vector

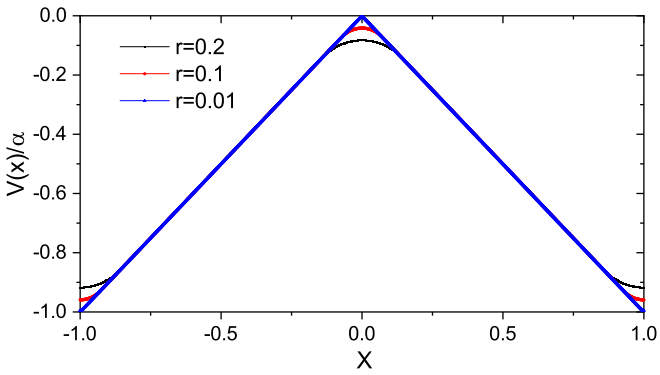

FIG. 1. Shape of the potential $V(x)$ for the round-off triangle map, at different values of r.

$\binom{\delta x_n}{\delta p_n}$ increases significantly only when a trajectory reaches the neighborhood of $x = 0$ or $|x| = 1$, that is, when $|x| < \frac{\sqrt{2}}{2}r$ or $|x| > 1 - \frac{\sqrt{2}}{2}r$. We denote these two regions by E_0 and $E_{|1|}$, respectively, and $E = E_0 \cup E_{|1|}$. The width of E is $w_E = 2\sqrt{2}r$, so that the average time between consecutive passages of a trajectory through E is $\overline{\tau} \simeq \frac{\sqrt{2}}{2r}$. For consecutive passages at time steps $t = n$ and $t = n + \tau$, in the case of small r we have [46]

$$\begin{pmatrix} \delta x_{n+\tau} \\ \delta p_{n+\tau} \end{pmatrix} = \begin{bmatrix} \frac{\sqrt{2}\alpha}{r} & \frac{\sqrt{2}\alpha}{r}(\tau - 1) \\ \frac{\sqrt{2}\alpha}{r} & \frac{\sqrt{2}\alpha}{r}(\tau - 1) \end{bmatrix} \begin{pmatrix} \delta x_n \\ \delta p_n \end{pmatrix}. \tag{4}$$

Given the distribution of return times τ to the region E, $P(\tau) = q_r^{\tau-1} p_r$, where $p_r = w_E/2 = \sqrt{2}r$ and $q_r = 1 - p_r$, we obtain [46]

$$\begin{aligned} \lambda_{\mathrm{lyp}} &= \frac{\sum_{\tau=1}^{\infty} q_r^{\tau-1} p_r \ln\left(\frac{\sqrt{2}\alpha}{r}\tau\right)}{\overline{\tau}} \\ &= 2r^2 \sum_{\tau=1}^{\infty} (1 - \sqrt{2}r)^{\tau-1} \ln\left(\frac{\sqrt{2}\alpha}{r}\tau\right). \end{aligned} \tag{5}$$

Note that λ_{lyp} decreases with r, and $\lambda_{\mathrm{lyp}} \to 0$ when $r \to 0$. As shown in Fig. 2, this analytical estimate is in very good agreement with the numerically computed Lyapunov exponent.

Similarly, we can also estimate the largest *local* Lyapunov exponent $\lambda_{\mathrm{lyp}}^{\max}$ for the region E:

$$\lambda_{\mathrm{lyp}}^{\max} = \ln\left(\frac{\sqrt{2}\alpha}{r}\right). \tag{6}$$

In contrast with the Lyapunov exponent, $\lambda_{\mathrm{lyp}}^{\max}$ increases as r decreases. If we consider the dynamics up to time t, the proportion of trajectories that satisfy $x(t') \in E$ for all t' up to some time t is equal to $(\sqrt{2}r)^t$, i.e., it decreases exponentially with time.

Exponential growth of OTOC. In order to study the quantum evolution we consider the Floquet operator

$$U = \exp\left(-i\frac{\hat{p}^2}{2\hbar}\right) \exp\left(-i\frac{V(\hat{x})}{\hbar}\right), \tag{7}$$

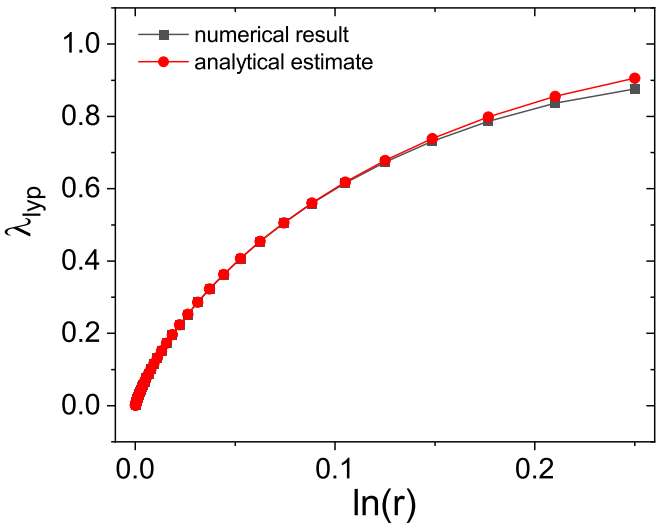

FIG. 2. Lyapunov exponent $\lambda_{\rm lyp}$ as a function of r. The analytical estimate of Eq. (5) is compared with the numerical results. Here and in the following figures, $\alpha = [(\sqrt{5}-1)/2 - e]/2$.

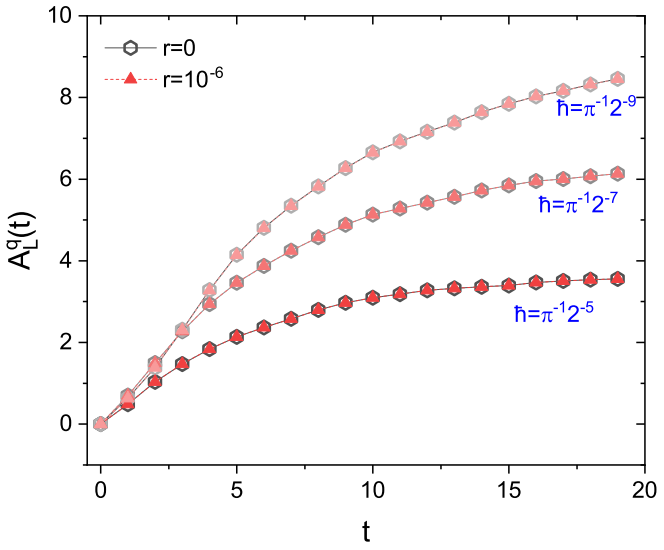

FIG. 3. Average OTOC $A_L^q(t)$ for different values of $\hbar$, at $r = 0$ and 10^{-6}. It can be seen that, for the values of $\hbar$ considered here, the growth rate increases with decreasing $\hbar$. Data for $r = 10^{-6}$ are almost indistinguishable from those at $r = 0$, as expected since in quantum mechanics the sharp, nonanalytic features of the triangle-map potential $V(x)$ are smoothed.

where $\hbar = \frac{2}{\pi D}$, D being the Hilbert space dimension. Here, we consider the averaged OTOC defined as follows [47],

$$A_L^q(t) = \frac{1}{N}\sum_{k=1}^{N} \ln(\langle\psi_k|[\hat{x}(t), \hat{p}(0)]^2|\psi_k\rangle/\hbar^2), \tag{8}$$

where $|\psi_k\rangle$ is the initial coherent state, which, in the position basis, reads as follows:

$$\psi_k(x) = (\pi\hbar)^{-1/4} \exp\left(-\frac{(x-x_k)^2}{2\hbar} + \frac{ip_k x}{\hbar}\right). \tag{9}$$

Here, (x_k, p_k) is the center of the kth initial state.

In Fig. 3, we show that the initial growth of the quantum OTOC is exponential also for the classically nonchaotic case ($r = 0$), for which the Lyapunov exponent $\lambda_{\rm lyp} = 0$. Therefore, as in polygons, one can observe that quantum mechanics induces short-time exponential instability in a classically nonchaotic model. We plot in Fig. 3 the quantum OTOC for three different values of $\hbar$. We can see that, in agreement with Fig. 4 of Ref. [40], the quantum OTOC grows exponentially with a rate which increases as $\hbar$ is decreased [48]. This appears to be the *experimentum crucis* which proves the breakdown of the correspondence principle. However, as we shall discuss below, a deeper analysis leads to a quite different conclusion.

Quantum-to-classical correspondence. In order to study the quantum-to-classical correspondence, we consider the canonical substitution $[\hat{x}(t), \hat{p}(0)] \to i\hbar\{x(t), p(0)\}_{\rm PB}$, where PB stands for Poisson brackets. We thus obtain the classical counterpart of OTOC as [49,50]

$$A_L^c(t) = \frac{1}{N}\sum_{k=1}^{N} \ln\left[\int d\boldsymbol{\gamma}\rho_{\boldsymbol{\gamma}_0^k}(\boldsymbol{\gamma})\left(\frac{\partial x(t)}{\partial x(0)}\right)^2\right], \tag{10}$$

where $\gamma = (x, p)$. The initial condition is a Gaussian distribution

$$\rho_{\boldsymbol{\gamma}_0^k}(\boldsymbol{\gamma}) = (2\pi\sigma^2)^{-1} \exp\left(-\frac{(x-x_k)^2 + (p-p_k)^2}{2\sigma^2}\right), \tag{11}$$

where, in order to compare with the quantum wave packet, we take $\sigma = \sqrt{\frac{\hbar_c}{2}}$ and $\hbar_c = \hbar$.

There are obviously no problems for the correspondence principle when $r > 0$. The round-off triangle map is chaotic and therefore one expects that classical and quantum OTOC agree up to the Ehrenfest time. This is nicely confirmed by our numerical computations (see Supplemental Material [46]) where one can see that the growth rate of $A_L^c(t)$ approaches the Lyapunov exponent as $\hbar$ goes to zero while $A_L^q(t)$ approaches the corresponding $A_L^c(t)$ up to the Ehrenfest time.

On the other hand, the case $r = 0$ requires careful inspection. First of all, we observe that there are singular points (the cusps in the potential) for which $\partial x(t)/\partial x(0)$ diverges. This leads to a divergence of the growth rate for A_L^c, as explained in what follows.

Besides A_L^c, we consider two other ways of averaging over initial conditions:

$$L_A^c(t) = \ln\left[\frac{1}{N}\sum_{k=1}^{N}\int d\boldsymbol{\gamma}\rho_{\boldsymbol{\gamma}_0^k}(\boldsymbol{\gamma})\left(\frac{\partial x(t)}{\partial x(0)}\right)^2\right], \tag{12}$$

and

$$L_L^c(t) = \frac{1}{N}\sum_{k=1}^{N}\int d\boldsymbol{\gamma}\rho_{\boldsymbol{\gamma}_0^k}(\boldsymbol{\gamma}) \ln\left(\frac{\partial x(t)}{\partial x(0)}\right)^2. \tag{13}$$

We can see that L_L^c is an average of the quantity considered in computing the Lyapunov exponent. For a number N of initial conditions large enough, we can expect that

$$L_L^c(t) \propto 2\lambda_{\rm lyp} t. \tag{14}$$

As for $L_A^c(t)$, it is close to $L_L^c(t)$ only if the fluctuations from trajectory to trajectory of the local Lyapunov exponent are quite small. On the other hand, for small r such fluctuations

are large and $L_A^c(t)$ is dominated by the trajectories with the largest local Lyapunov exponent $\lambda_{\rm lyp}^{\rm max}$. Given $\lambda_{\rm lyp}^{\rm max}$ from Eq. (6), and the fraction $(\sqrt{2}r)^t$ of the trajectories with the largest local Lyapunov exponent up to time t, we conclude that, for $r \to 0$,

$$L_A^c(t) \propto 2\lambda_{\rm lyp}^* t, \tag{15}$$

where

$$\lambda_{\rm lyp}^* \approx \ln\left(\frac{\sqrt{2}\alpha}{r}\right) + \frac{1}{2}\ln(\sqrt{2}r). \tag{16}$$

Therefore, the growth rate of L_A^c diverges when $r \to 0$, in spite of the fact that in that limit the system is classically integrable.

Then we come to the discussion of the quantity $A_L^c(t)$. For sufficiently small $\hbar_c$, for each single initial ensemble at small times all the trajectories remain very close, at distances much smaller than r. Then the behavior of $A_L^c(t)$ is quite similar to that of $L_L^c(t)$. On the other hand, for longer times, when the size of the ensemble becomes much larger than r, $A_L^c(t)$ is close to $L_A^c(t)$. As a conclusion, for $\sigma = \sqrt{\frac{\hbar}{2}} \ll r$ we obtain

$$A_L^c(t) \propto \begin{cases} L_L^c(t) \propto 2\lambda_{\rm lyp} t, & t \ll t^*, \\ L_A^c(t) \propto 2\lambda_{\rm lyp}^* t, & t \gg t^*, \end{cases} \tag{17}$$

where t^* indicates the timescale when the size $\Delta X(t) \sim \sqrt{\hbar_c}\exp(\lambda_{\rm lyp} t)$ of the wave packet becomes comparable with r.

Therefore, we can estimate the value of t^* as

$$t^* \sim \frac{1}{\lambda}\ln\frac{r}{\sqrt{\hbar_c}}. \tag{18}$$

For a fixed r, when $\hbar_c$ is large, t^* is very small, and $A_L^c(t)$ increases with growth rate $2\lambda_{\rm lyp}^*$. On the other hand, for $\hbar_c \to 0$ we have $t^* \to \infty$, and the initial growth rate is given by $2\lambda_{\rm lyp}$ (see Supplemental Material [46] for a numerical confirmation of the above picture).

To examine the validity of the correspondence principle for $r = 0$, we first compute the quantum OTOC $A_L^q(t)$ at different values of $\hbar$. Numerical results are shown in Fig. 4(a). It is clear that the growth rate of A_L^q, which we have seen to increase with decreasing $\hbar$ (down to $\hbar = \pi^{-1}2^{-9}$), vanishes instead when $\hbar \to 0$, in accordance with the correspondence principle.

For a detailed classical-quantum comparison, given that quantum mechanics smoothens the sharp features of the classical potential below the Planck's scale, we juxtapose the quantum results for OTOC at $r = 0$ with the classical ones at $r = 1/\sqrt{D}$. As shown in Fig. 4(b), also the growth rate of $AL_c^{\rm tan}$ vanishes when $\hbar_c \to 0$. In order to get a clear picture of the difference between the quantum and classical results, we consider the relative difference of A_L^q and A_L^c,

$$\Delta_{qc}(t) = \left|A_L^q(t) - A_L^c(t)\right| / \left[A_L^q(t) + A_L^c(t)\right]. \tag{19}$$

The results for $t = t_0 = 6, 10$ are shown in Fig. 4(c). It is clear that in both cases $\Delta_{qc} \to 0$ with decreasing $\hbar$. These results show that there is no breakdown of the correspondence principle.

It is intriguing that the OTOC growth rate exhibits a nonmonotonous dependence on $\hbar$. While we do not have a rigorous explanation for this numerical result, a possible clue

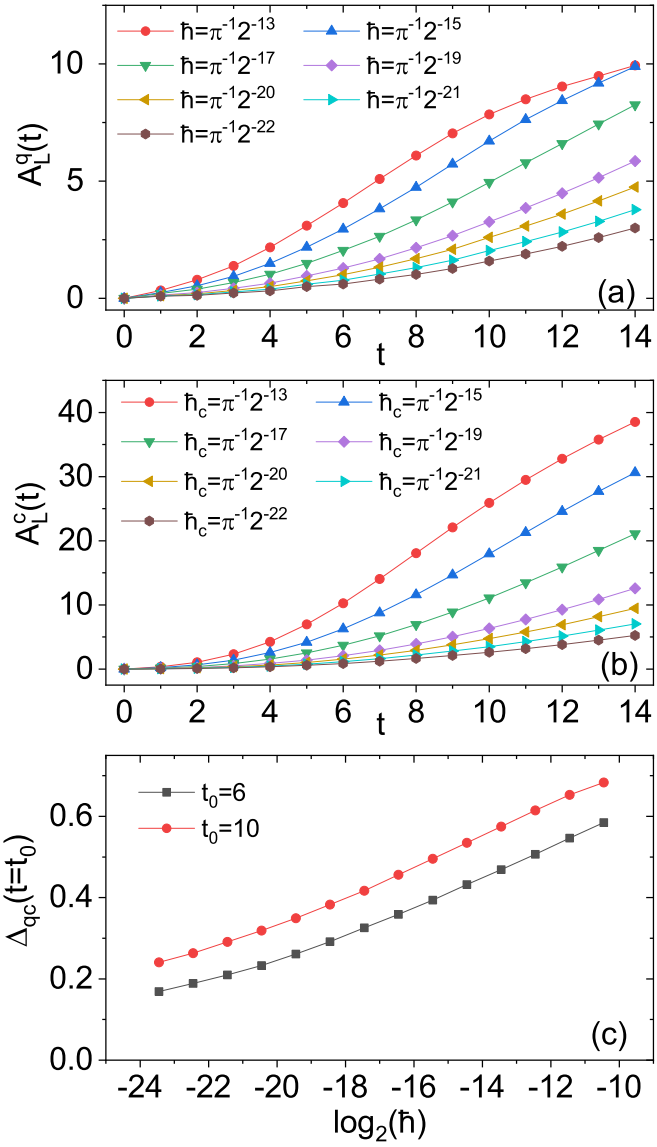

FIG. 4. $A_L(t)$ in (a) a quantum case for $r = 0$ and (b) its classical counterpart for different $\hbar$ from $\hbar = \pi^{-1}2^{-13}$ to $\hbar = \pi^{-1}2^{-22}$. The classical counterpart $A_L^c(t)$ is obtained by considering a finite r, which is related to the dimension D of the system as $r = \frac{1}{\sqrt{D}}$. (c) Difference between $A_L^q(t)$ and $A_L^c(t)$ at a fixed time t_0, denoted by $\Delta_{qc}(t = t_0)$, for $t_0 = 6$ (black blocks) and $t_0 = 10$ (red circles).

is the following. Due to the finite size of the wave packet, the quantum system "sees" a rounded potential, with an effective radius $r = f(\hbar)$, where f is a monotonous growing function of $\hbar$. We then have, as we have discussed for the classical case, a growth rate $2\lambda_{\rm lyp}$ up to a time $t^\star$ and then a growth rate $2\lambda_{\rm lyp}^\star$. Numerical data as well as Eq. (18) suggest that $t^\star$ increases when $\hbar$ decreases, in such a way that the initial growth rate is determined by the fluctuations in the local Lyapunov exponent for large $\hbar$, and by the Lyapunov exponent for small $\hbar$. In particular, the OTOC growth rate in Fig. 3 is not given by the Lyapunov exponent.

Conclusions. In recent years, the OTOC has emerged as an important tool to characterize chaos in many-body quantum systems. This validity, first corroborated by models which

exhibit an exponential increase of OTOC with a rate equal to twice the Lyapunov exponent of the underlying classical dynamics, has been more recently questioned. Indeed, unstable fixed points might lead to an exponential increase of OTOC even in integrable systems [37,38]. Even more importantly, the exponential increase can be observed at early times, questioning the validity of the correspondence principle [40]. Our results show that the correspondence principle is restored and the OTOC remains a useful diagnosis of chaotic dynamics, provided an appropriate average over initial states is done and singularities in the potential are rounded off below the scale of Planck's cell.

Acknowledgments. J.W. and W.-g.W. acknowledge the Natural Science Foundation of China under Grants No. 11535011 and No. 11775210. G.B. acknowledges the financial support of the INFN through the project "QUANTUM."

[1] G. P. Berman and G. M. Zaslavsky, Physica A **91**, 450 (1978); M. Toda and K. Ikeda, Phys. Lett. A **124**, 165 (1987); Y. Gu, *ibid.* **149**, 95 (1990).
[2] G. Casati, B. V. Chirikov, I. Guarneri, and D. L. Shepelyansky, Phys. Rev. Lett. **56**, 2437 (1986).
[3] G. Casati, B. V. Chirikov, F. M. Izrailev, and J. Ford, in *Stochastic Behavior in Classical and Quantum Hamiltonian Systems*, Lecture Notes in Physics Vol. 93 (Springer, Berlin, 1979), p. 334.
[4] B. V. Chirikov, F. M. Izrailev, and D. L. Shepelyansky, Sov. Scient. Rev. C **2**, 209 (1981).
[5] G. Casati and B. V. Chirikov, *Quantum Chaos: Between Order and Disorder* (Cambridge University Press, Cambridge, UK, 1995).
[6] A. Larkin and Y. N. Ovchinnikov, Zh. Eksp. Teor. Fiz. **55**, 2262 (1968) [JETP **28**, 1200 (1969)].
[7] A. Kitaev, Hidden correlations in the Hawking radiation and thermal noise, talk given at KITP, Santa Barbara, 2014, http://online.kitp.ucsb.edu/online/joint98/kitaev/.
[8] J. Maldacena and D. Stanford, Phys. Rev. D **94**, 106002 (2016).
[9] J. Maldacena, S. H. Shenker, and D. Stanford, J. High Energy Phys. 08 (2016) 106.
[10] P. Hosur, X.-L. Qi, D. A. Roberts, and B. Yoshida, J. High Energy Phys. 02 (2016) 004.
[11] Y. Huang, Y.-L. Zhang, and X. Chen, Ann. Phys. **529**, 1600318 (2017).
[12] B. Swingle, G. Bentsen, M. Schleier-Smith, and P. Hayden, Phys. Rev. A **94**, 040302(R) (2016).
[13] E. B. Rozenbaum, S. Ganeshan, and V. Galitski, Phys. Rev. Lett. **118**, 086801 (2017).
[14] K. Hashimoto, K. Muratab, and R. Yoshii, J. High Energy Phys. 10 (2017) 138.
[15] I. Kukuljan, S. Grozdanov, and T. Prosen, Phys. Rev. B **96**, 060301(R) (2017).
[16] R. Fan, P. Zhang, H. Shen, and H. Zhai, Sci. Bull. **62**, 707 (2017).
[17] M. Giärttner, J. G. Bohnet, A. Safavi-Naini, M. L. Wall, J. J. Bollinger, and A. M. Rey, Nat. Phys. **13**, 781 (2017).
[18] J. Li, R. Fan, H. Wang, B. Ye, B. Zeng, H. Zhai, X. Peng, and J. Du, Phys. Rev. X **7**, 031011 (2017).
[19] J. S. Cotler, D. Ding, and G. R. Penington, Ann. Phys. **396**, 318 (2018).
[20] C.-J. Lin and O. I. Motrunich, Phys. Rev. B **97**, 144304 (2018).
[21] I. García-Mata, M. Saraceno, R. A. Jalabert, A. J. Roncaglia, and D. A. Wisniacki, Phys. Rev. Lett. **121**, 210601 (2018).
[22] S. Pappalardi, A. Russomanno, B. Žunkovič, F. Iemini, A. Silva, and R. Fazio, Phys. Rev. B **98**, 134303 (2018).
[23] K. X. Wei, C. Ramanathan, and P. Cappellaro, Phys. Rev. Lett. **120**, 070501 (2018).
[24] A. Das, S. Chakrabarty, A. Dhar, A. Kundu, D. A. Huse, R. Moessner, S. S. Ray, and S. Bhattacharjee, Phys. Rev. Lett. **121**, 024101 (2018).
[25] J. Rammensee, J. D. Urbina, and K. Richter, Phys. Rev. Lett. **121**, 124101 (2018).
[26] C. W. von Keyserlingk, T. Rakovszky, F. Pollmann, and S. L. Sondhi, Phys. Rev. X **8**, 021013 (2018).
[27] A. Nahum, S. Vijay, and J. Haah, Phys. Rev. X **8**, 021014 (2018).
[28] V. Khemani, A. Vishwanath, and D. A. Huse, Phys. Rev. X **8**, 031057 (2018).
[29] T. Rakovszky, F. Pollmann, and C. W. von Keyserlingk, Phys. Rev. X **8**, 031058 (2018).
[30] J. Chávez-Carlos, B. López-del-Carpio, M. A. Bastarrachea-Magnani, P. Stránský, S. Lerma-Hernández, L. F. Santos, and J. G. Hirsch, Phys. Rev. Lett. **122**, 024101 (2019).
[31] E. M. Fortes, I. García-Mata, R. A. Jalabert, and D. A. Wisniacki, Phys. Rev. E **100**, 042201 (2019).
[32] F. Borgonovi, F. M. Izrailev, and L. F. Santos, Phys. Rev. E **99**, 052143 (2019).
[33] R. Prakash and A. Lakshminarayan, Phys. Rev. B **101**, 121108(R) (2020).
[34] P. D. Bergamasco, G. G. Carlo, and A. M. F. Rivas, Phys. Rev. Research **1**, 033044 (2019).
[35] K. X. Wei, P. Peng, O. Shtanko, I. Marvian, S. Lloyd, C. Ramanathan, and P. Cappellaro, Phys. Rev Lett. **123**, 090605 (2019).
[36] M. Niknam, L. F. Santos, and D. G. Cory, Phys. Rev. Research **2**, 013200 (2020).
[37] S. Pilatowsky-Cameo, J. Chávez-Carlos, M. A. Bastarrachea-Magnani, P. Stránský, S. Lerma-Hernández, L. F. Santos, and J. G. Hirsch, Phys. Rev. E **101**, 010202(R) (2020).
[38] T. Xu, T. Scaffidi, and X. Cao, Phys. Rev. Lett. **124**, 140602 (2020).
[39] S. Xu and B. Swingle, Nat. Phys. **16**, 199 (2020).
[40] E. B. Rozenbaum, L. A. Bunimovich, and V. Galitski, Phys. Rev. Lett. **125**, 014101 (2020).
[41] X. Chen and T. Zhou, arXiv:1804.08655.
[42] R. Hamazaki, K. Fujimoto, and M. Ueda, arXiv:1807.02360.
[43] J. Wang, G. Benenti, G. Casati, and W.-g. Wang, Phys. Rev. Research **2**, 043178 (2020).
[44] M. Jammer, *The Conceptual Development of Quantum Mechanics* (McGraw-Hill, New York, 1966).
[45] G. Casati and T. Prosen, Phys. Rev. Lett. **85**, 4261 (2000).

[46] See Supplemental Material at http://link.aps.org/supplemental/10.1103/PhysRevE.103.L030201 for details on the analytical estimate of the Lyapunov exponent, different ways of averaging over initial conditions, and an example of quantum-classical correspondence for OTOC at $r > 0$.

[47] The operators $\hat{x}$ and $\hat{p}$ used to compute the OTOC are defined as in Ref. [21]. Such construction, in terms of Schwinger shift operators, avoids problems related to the definition of $\hat{x}$ and $\hat{p}$ on the quantized torus, which is equivalently to consider the operator $\sin \pi \hat{x}$ and $\sin \pi \hat{p}$ instead. So what is actually studied here is the following quantity: $AL_q(t) = \frac{1}{N} \sum_{k=1}^{N} \ln \left(\langle \psi_k | \{ \sin[\pi \hat{x}(t)], \sin[\pi \hat{p}(0)] \}^2 | \psi_k \rangle / \hbar^2 \right)$.

[48] To be precise, in Ref. [40] the apparent violation of the correspondence principle was discussed for a different averaging, that is, first averaging the OTOC and then taking the logarithm, rather than averaging the logarithm of OTOC. While these two averages, denoted in our Letter as *LA* and *AL*, lead to qualitatively similar results for large $\hbar$, their behavior at small $\hbar$ is very different, as explained later in our Letter. While the correspondence principle remains valid also for *AL*, the growth rate for this quantity is dominated by the strong fluctuations of OTOC due to the presence of singular points in the potential. Here, we focus instead on *AL* since the growth rate for this quantity is twice the Lyapunov exponent of the classical underlying dynamics. For this reason, *AL* rather than *LA* is a diagnostic of chaotic dynamics.

[49] The superscript "tan" refers to the fact that in computing the OTOC we use the tangent map rather than evolving two nearby trajectories and computing their distance $\delta x(t)$.

[50] Given the definition of $\hat{x}$ and $\hat{p}$ explained in Ref. [47], we actually compute $AL_c^{\tan}(t) = \frac{1}{N} \sum_{k=1}^{N} \ln \left(\pi^2 \int d\boldsymbol{\gamma} \rho_{\boldsymbol{\gamma}_0^k}(\boldsymbol{\gamma}) (\cos[\pi x(t)] \cos[\pi p(0)] \frac{\partial x(t)}{\partial x(0)})^2 \right)$.